Impaired LAIR-1-mediated immune control due to collagen degradation in fibrosis

Tiago Carvalheiro[1,2,3], Wioleta Marut[1,2], M. Inês Pascoal Ramos[1,3], Samuel García[1,2,4], Devan Fleury[5], Alsya J. Affandi[1,2], Aniek S. Meijers[1], Barbara Giovannone[1,6], Ralph G. Tieland[1,2], Eline Elshof[1,3], Andrea Ottria[1,2], Marta Cossu[1,2], Matthew L. Meizlish[7], Tineke Veenendaal[8], Meera Ramanujam[5], Miguel E. Moreno-García[5], Judith Klumperman[8], Nalan Liv[8], Timothy R.D.J. Radstake[1,2], Linde Meyaard[1,3,9*]

[1]Center for Translational Immunology, University Medical Center Utrecht, Utrecht University, Utrecht, The Netherlands

[2]Department of Rheumatology & Clinical Immunology, University Medical Center Utrecht, Utrecht University, Utrecht, The Netherlands

[3]Oncode Institute, Utrecht, The Netherlands

[4]Rheumatology & Immuno-mediated Diseases Research Group (IRIDIS), Galicia Sur Health Research Institute (IIS Galicia Sur), SERGAS-UVIGO, Vigo, Spain

[5]Immunology and Respiratory Diseases Research, Boehringer Ingelheim, Ridgefield, CT, USA

[6]Department of Dermatology, University Medical Center Utrecht, Utrecht University, Utrecht, The Netherlands

[7]Howard Hughes Medical Institute, Department of Immunobiology, Yale University School of Medicine, New Haven, CT, USA

[8]Cell Biology, Centre for Molecular Medicine, University Medical Center Utrecht, Utrecht University, Utrecht, The Netherlands

[9]Lead contact

***Correspondence:**

Prof. Dr. Linde Meyaard

email: l.meyaard@umcutrecht.nl

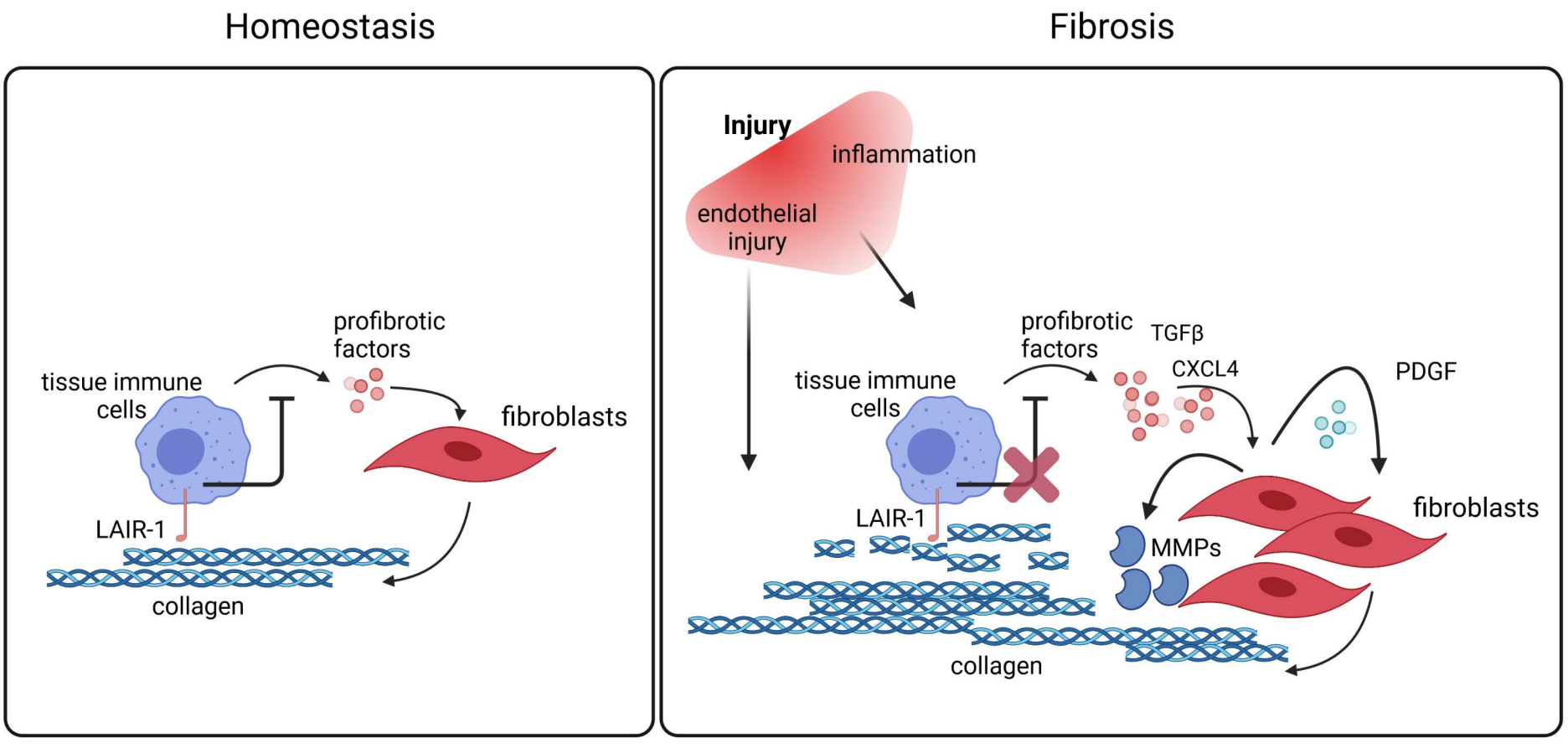
Homeostasis
Fibrosis
tissue immune cells
profibrotic factors
fibroblasts
LAIR-1
collagen
Injury
inflammation
endothelial injury
tissue immune cells
profibrotic factors
TGFβ
CXCL4
PDGF
fibroblasts
LAIR-1
MMPs
collagen

Summary

Tissue repair is disturbed in fibrotic diseases like systemic sclerosis (SSc), where the deposition of large amounts of extracellular matrix components such as collagen interferes with organ function. LAIR-1 is an inhibitory collagen receptor highly expressed on tissue immune cells. We questioned whether in SSc, impaired LAIR-1-collagen interaction is contributing to the ongoing inflammation and fibrosis.

We found that SSc patients do not have an intrinsic defect in LAIR-1 expression or function. Instead, fibroblasts from SSc patients deposit disorganized collagen products *in vitro*, which are dysfunctional LAIR-1 ligands. This can be mimicked in healthy fibroblast stimulated by soluble factors that drive inflammation and fibrosis in SSc and is dependent of matrix metalloproteinases and platelet-derived growth factor receptor signaling.

In support of a non-redundant role of LAIR-1 in the control of fibrosis, we found that LAIR-1-deficient mice have increased skin fibrosis in the bleomycin mouse model for SSc. Thus, LAIR-1 represents an essential control mechanism for tissue repair. In fibrotic disease, excessive collagen degradation may lead to a disturbed feedback loop. The presence of functional LAIR-1 in patients provides a therapeutic opportunity to reactivate this intrinsic negative feedback mechanism in fibrotic diseases.

Key words: Fibrosis, Systemic Sclerosis, LAIR-1, CD305, Collagen, Tissue repair

Introduction

The extracellular matrix (ECM) is a dynamic structure, in which production and deposition are finely balanced with degradation and removal, regulated through pro-fibrotic factors, matrix metalloproteinases (MMPs) and other collagenases. Tightly controlled ECM homeostasis is essential for healthy connective tissues (Lu et al., 2011; Meizlish et al., 2021). Tissue repair after injury entails a cascade of inflammation, repair and ultimately resolution. Tissue resident macrophages can sense ECM composition. Signals from damaged tissue initiate a dynamic process that involves the recruitment of immune cells, which help to induce fibroblast differentiation into myofibroblasts, which in turn deposit ECM to repair the tissue. Finally, myofibroblasts are eliminated and the ECM is degraded and remodeled, in order to resolve the repair process (Meizlish *et al.*, 2021; Okabe and Medzhitov, 2016).

Fibrosis is an abnormal reparative process that is characterized by excessive ECM deposition without reciprocal degradation (Henderson et al., 2020). This progressive accumulation of ECM results in remodeling of the tissue architecture and can lead to organ failure (Distler et al., 2019; Weiskirchen et al., 2019). The fibrotic scar consists predominantly of fibrilar collagens (types I and III), fibronectin and basement-membrane proteins such as type IV collagen and laminin (Karsdal et al., 2017; Theocharis et al., 2016; Wynn, 2008). Complex cellular and molecular processes drive fibrosis, with transforming growth factor β (TGFβ) family proteins playing a central role by stimulating the synthesis of ECM proteins by effector cells such as myofibroblasts (Lodyga and Hinz, 2020; Rockey et al., 2015).

Systemic sclerosis (SSc) is a prototypical immune-mediated fibrotic disease, characterized by vasculopathy, inflammation and fibrosis of the skin and internal organs. The etiology of SSc is largely unknown and patients can present with a wide range of clinical manifestations, resulting in high morbidity and mortality (Denton and Khanna, 2017). Typically, immune cell infiltration into skin and internal organs occurs early in the disease, prior to the onset of fibrosis. Immune mediators such as TGFβ - namely TGFβ2, type I interferon (IFN), platelet-derived growth factor (PDGF), IL-6 and type 2 cytokines (including IL-4, IL-10 and IL-13) are considered central to the pathogenesis of SSc (Allanore et al., 2015; Kania et al., 2019). In addition, the chemokine CXCL4 is increased in the circulation and skin of SSc patients and

correlates with the presence and progression of complications such as lung fibrosis and pulmonary arterial hypertension (van Bon et al., 2014).

ECM proteins interact with different cell types through cell surface receptors, including integrins, receptor tyrosine kinases, and immunoglobulin-like receptors (Zeltz and Gullberg, 2016). Leukocyte associated immunoglobulin-like receptor-1 (LAIR-1; CD305) is an Immunoreceptor Tyrosine-based Inhibitory Motif (ITIM)-bearing inhibitory receptor for collagen, broadly expressed on most immune cells (Lebbink et al., 2006; Meyaard et al., 1997). Activation of LAIR-1 *in vitro* potently inhibits diverse immune cells such as T cells, NK cells (Jansen et al., 2007; Maasho et al., 2005; Meyaard *et al.*, 1997; Park et al., 2020), B cells (Merlo et al., 2005) plasmacytoid dendritic cells (pDC) (Bonaccorsi et al., 2010; Son et al., 2012) and monocytes (Carvalheiro et al., 2020; Keerthivasan et al., 2021; Son and Diamond, 2015). LAIR-1 inhibitory function can be regulated at the membrane expression level and by the natural soluble agonists soluble-LAIR-1 (sLAIR-1), a shed form of LAIR-1, and LAIR-2. LAIR-2 is a soluble protein, homologous to human LAIR-1, lacking the transmembrane and intracellular domain, with a higher affinity for collagens than LAIR-1, thereby blocking LAIR-1 ligation to collagen (Lebbink et al., 2008).

LAIR-1 is expressed on immune cells in healthy skin, where it can interact with collagens (Carvalheiro *et al.*, 2020; Lebbink *et al.*, 2006). It recognizes multiple collagens and collagen-domain containing proteins. Collagens have multiple functional binding sites for LAIR-1, the glycine-proline-hydroxyproline content of collagen domains appears to be the dominant determinant for LAIR-1 binding (Lebbink *et al.*, 2006; Lebbink et al., 2009). In fibrotic tissues such as those in SSc patients, there should be abundant amounts of collagen to be sensed by LAIR-1 on tissue immune cells, yet inflammation continues. We here questioned whether in SSc, impaired LAIR-1-collagen interaction is contributing to the ongoing inflammation and fibrosis.

Results

LAIR-1 expression and its intrinsic function is normal in SSc patients

We first investigated whether the function of LAIR-1 is impaired in patients with SSc. We first determined LAIR-1 expression on circulating immune cells from SSc patients and healthy controls (HC) by flow cytometry. LAIR-1 expression at the cell surface was comparable between SSc patients and HC on type-2 conventional dendritic cells (cDC2), plasmacytoid dendritic cells (pDCs), $CD4^+$ and $CD8^+$ T cells, NK cells and B cells and on most monocyte subsets. In classical monocytes, LAIR-1 expression was significantly increased in SSc patients compared to HC (Figure 1A). As described before (Carvalheiro *et al.*, 2020), LAIR-1 was not expressed on type-1 conventional dendritic cells (cDC) (data not shown).

In affected skin of SSc patients, available profiling data by array [GSE95065] show that *LAIR1* gene expression was increased in the skin of SSc patients (Supplemental Figure 1A), probably reflecting an increase in immune cells, given the strong correlation between *LAIR1* expression and *PTPRC* (gene encoding CD45) and moderate correlation with the macrophage marker *CD68* (Supplemental Figure 1B). By immunohistochemistry, we confirmed that LAIR-1 was expressed in skin from HC and SSc patients, both in affected and non-affected skin (Figure 1B). Thus, LAIR-1 is expressed on circulating immune cells of SSc patients and in their tissues such as skin.

We next investigated whether LAIR-1 on immune cells from SSc patients retains its capacity to inhibit cellular activation. Monocytes and pDC from HC and SSc patients were stimulated with TLR ligands together with an antibody that acts as a LAIR-1 agonist. LAIR-1 activation in both groups caused a similar inhibition of IL-6 and TNF-α production by monocytes and IFN-α production by pDC (Figure 1C). Thus, the intrinsic inhibitory function of LAIR-1 is preserved in SSc patients.

We further explored whether soluble mediators in the circulation of SSc patients could block collagen interaction with cellular LAIR-1. For this purpose, labelled collagen was incubated with serum from SSc patients or HC after which collagen binding to a LAIR-1 overexpressing line was determined by flow cytometry. Serum from SSc patients and HC blocked collagen binding to LAIR-1 to a similar degree (Figure 1D, Supplemental Figure 2A). Consistent with this finding,

circulating concentrations of sLAIR-1 (Figure 1E) and LAIR-2 (Figure 1F) were not different between SSc patients and HC. Altogether, these experiments indicate that LAIR-1 is normally expressed, has preserved inhibitory capacity, and does not encounter higher levels of known LAIR-1 antagonists in SSc patients compared to HC.

LAIR-1 binds to *in vitro* and *in vivo* fibrotic ECM

We have previously shown that LAIR-1 is able to bind to collagen in healthy skin (Lebbink *et al.*, 2006). The fibrotic collagen present in the skin of SSc patients is structurally different from that found in healthy skin, with dense, aligned dermal collagen bundles (Varga and Trojanowska, 2008), which potentially could affect LAIR-1 binding. However, we observed that LAIR-1 binding to both HC and SSc skin samples was comparable (Figure 2A).

Fibroblasts in the skin of SSc patients are constantly exposed to inflammatory and pro-fibrotic factors, such as TGFβ and CXCL4 (Allanore *et al.*, 2015). We mimicked these circumstances *in vitro* by culturing dermal fibroblasts obtained from HC and SSc patients in the presence of TGFβ or CXCL4 and visualized collagen I deposition by immunofluorescence. TGFβ treatment induced enhanced collagen I production compared to untreated (medium) cultures, and the collagen was deposited in characteristic aligned fibers, both in cultures of fibroblasts from SSc patients and from HC. In contrast, CXCL4 stimulation resulted in more disorganized collagen I, particularly in fibroblasts from SSc patients (Figure 2B). We assessed LAIR-1 binding to the deposited ECM using a hLAIR-1-IgG fusion protein (Lebbink *et al.*, 2006). We observed that LAIR-1 efficiently bound to the ECM produced by fibroblasts from both HC and SSc patients, both in non-stimulated and stimulated conditions. However, when compared to HC, SSc dermal fibroblasts stimulated with CXCL4 produced an increased amount of dense, non-fibrilar shaped structures that bound LAIR-1 but did bind collagen I antibodies (Figure 2B). Thus, SSc fibroblasts stimulated with CXCL4, produce an ECM structure that is not collagen I and binds LAIR-1.

We next determined whether HC dermal fibroblasts stimulated with the potent pro-fibrotic combination of TGFβ and CXCL4 induced similar LAIR-1 binding structures as observed in SSc fibroblasts treated with CXCL4 only. Indeed, after stimulation with TGFβ and CXCL4, HC fibroblasts deposited similar dense structures binding LAIR-1 but not collagen I antibodies

(Figure 2C). The deposition of these structures increased evidently over time and was preferentially localized to decellularized areas (Figure 2C). Co-staining of the ECM with a pan-collagen mix of antibodies (recognizing collagen I, II, III, IV and V) revealed these structures as collagen, even though they did not have a typical fibrilar collagen conformation (Figure 2D). In addition, we confirmed that these structures do not bind to human Signal inhibitory receptor on leukocytes-1 (hSIRL-1), a protein with homology to LAIR-1, as an irrelevant binding control (Supplemental Figure 3A).

To study these fibrotic collagen structures at the nanoscale, fibroblast were stimulated with TGFβ2 and CXCL4 for electron microscopy (EM). High-resolution TEM images showed that the ECM of the non-stimulated (medium) condition was composed mostly of aligned collagen fibers that are homogenously interspaced and run parallel to each other (Figure 2E). In contrast, collagen fibers in the ECM produced by fibroblasts stimulated with TGFβ2 and CXCL4 were more frequently disorganized, had unidirectional orientation, and sometimes formed dense bundles (Figure 2E- black arrows and Supplemental Figure 4A-B). The disrupted organization of collagen fibers upon TGFβ2 and CXCL4 treatment can possibly be a consequence of the degradation of collagen fibers or collagen associated proteins responsible of their organization.

Since degraded and fragmented collagen triple helices may become unstable and spontaneously unfold, leaving denatured collagen fragments, we next assessed whether the LAIR-1 binding structures correspond to denatured collagen. We used a collagen hybridizing peptide (CHP), which specifically binds to denatured collagen strands by re-forming a triple-helical structure (Hwang et al., 2017). CHP did bind in cell-dense areas where collagen is actively produced, but did not co-localize with the LAIR-1-binding collagen structures (Figure 2F). This suggests that the collagen triple helical conformation is intact in the degraded fibers, in agreement for a need of a triple helical conformation for LAIR-1 binding (Lebbink *et al.*, 2006; Lebbink *et al.*, 2009). Thus, fibroblasts stimulated with TGFβ and CXCL4 deposit dense structures consisting of degraded triple helical collagen in decellularized areas.

PDGF receptor signaling and Matrix Metalloproteinases are required for deposition of fibrotic LAIR-1 binding structures

The areas where the LAIR-1-binding dense collagen structures were deposited in *in vitro* cultures were devoid of cells (Figure 2C). By live cell imaging, we observed that the combination of TGFβ with CXCL4 drastically altered the motility of both HC and SSc dermal fibroblasts. Instead of forming an intact cellular monolayer, fibroblasts became highly motile, losing contact inhibition and forming multicellular layers, while leaving behind large decellularized areas (Figure 3A and Supplemental video 1-2).

Since PDGF signaling regulates proliferation and cell motility (Andrae et al., 2008), we next assessed whether this pathway could be involved in the production of the fibrotic LAIR-1 binding structures. Indeed, PDGF receptor inhibition in fibroblasts stimulated with TGFβ plus CXCL4 reduced cell motility and prevented the formation of multicellular layers of fibroblasts and the occurrence of decellularized areas (Supplemental video 3-6), as well as of the deposition of LAIR-1-binding structures (Figure 3B). Thus, PDGF-mediated fibroblast activation is required for the formation of these fibrotic collagen structures.

Next, we tested whether matrix metalloproteinases (MMP) were involved in the generation of the fibrotic LAIR-1-binding structures. Inhibition of MMP activity in HC dermal fibroblasts stimulated with TGFβ plus CXCL4 reduced the amount of LAIR-1-binding ECM structures (Figure 3C), and decreased cell motility (Supplemental video 7-10). Thus, the deposition of the LAIR-1-binding fibrotic structures requires cell motility and loss of cell contact inhibition mediated by PDGF receptor signaling and collagen degradation by MMPs.

Fibrotic collagen products have impaired capacity to activate LAIR-1

While the fibrotic collagen structures that we identified bind to hLAIR-1-IgG, we wondered whether they are functional ligands that can activate cellular LAIR-1. To investigate the effect of degraded collagen on LAIR-1 activation, we first used gelatin, which is the product of alkaline digestion of collagen. hLAIR-1-IgG bound in a dose dependent manner to plate-bound purified collagen I and, to a lesser extent to gelatin (Figure 4A). Next, to assess the

capacity of gelatin to activate LAIR-1, we used a NFAT-GFP reporter cell line transfected with LAIR-1-CD3ζ, which expresses Green Fluorescent Protein (GFP) when LAIR-1 is activated (Lebbink *et al.*, 2006). Optimal LAIR-1-CD3ζ-induced GFP production was achieved at ~6 µg/mL of immobilized collagen I, while lower concentrations or higher concentrations resulted in a lower percentage of GFP expressing cells (Figure 4B). In contrast, gelatin did not induce GFP production at any of the concentrations tested, even at concentrations where hLAIR-1-hIg effectively bound (Figure 4A-B). These results suggest that degraded collagen can bind LAIR-1 but cannot activate LAIR-1.

To investigate whether the fibrotic ECM structures that we identified are functional ligands for LAIR-1, we performed the same reporter cell assay on ECM produced by fibroblasts stimulated with TGFβ and CXCL4. We were able to trigger GFP expression in approximately 24% of LAIR-1-CD3ζ reporter cells using purified human collagen immobilized in the same culture vessel used in our ECM culture system (Figure 4C). ECM produced by unstimulated fibroblasts triggered GFP expression in 16.25±3.07% of the LAIR-1-CD3ζ reporter cells. However, ECM produced by TGFβ plus CXCL4 stimulated cells only resulted in 7.54±1.27% of GFP+ LAIR-1-CD3ζ reporter cells, which is a 54% reduction in the capacity to activate LAIR-1 (Figure 4C-D). We additionally performed a live reporter cell assay on ECM produced by fibroblasts from HC and SSc patients after stimulation with TGFβ plus CXCL4. After 70 hours of culture, GFP positive reporter cells were detected in areas where intact collagen structures were present. In contrast, in the decellularized regions, where degraded hLAIR-1-IgG binding collagen structures are deposited, LAIR-1-CD3ζ reporter cells were not induced to express GFP (Figure 4E and Supplemental video 11-14). This indicates that, despite having the capacity to bind LAIR-1, these degraded collagen structures do not activate LAIR-1. The production of degraded collagen in fibrotic conditions such as SSc could thus lead to incapacitated LAIR-1 inhibitory function and immune cell control.

Absence of LAIR-1 leads to increased bleomycin-induced skin fibrosis in the SSc mouse model

To investigate if the absence of functional LAIR-1 signaling would indeed lead to enhanced fibrosis similar to SSc, we subjected *Lair1*$^{-/-}$ mice to the bleomycin-induced fibrosis model. This

is a well-established mouse model of SSc, in which daily subcutaneous injections of bleomycin are used to induce skin fibrosis (Yamamoto et al., 1999). The model course can be divided into an inflammatory phase (7-15 days of bleomycin injections) and a fibrotic phase (2-4 weeks of bleomycin injections) (Figure 5A).

Untreated *Lair1*$^{-/-}$ mice did not display signs of skin fibrosis, as no differences were observed in skin thickness between *Lair1*$^{-/-}$ and WT mice measured by caliper (Figure 5B), and by histology (Supplemental Figure 5A-B). To determine whether LAIR-1 regulates the fibrotic process triggered upon bleomycin treatment, we subcutaneously injected bleomycin or sodium chloride (NaCl) as control in *Lair1*$^{-/-}$ or WT mice (Figure 5A). After 2 weeks of bleomycin treatment (inflammatory phase) *Lair1*$^{-/-}$ mice exhibited increased skin thickness compared to WT mice. Interestingly, *Lair1*$^{-/-}$ mice also showed increased skin thickness compared to WT mice after repeated injection of the vehicle NaCl (Figure 5C). This was accompanied by increased skin collagen content in *Lair1*$^{-/-}$ mice in both NaCl ($p<0.05$) and bleomcyin ($p=0.065$) treatment groups (Figure 5D).

In the fibrotic phase of this model, (4 weeks), *Lair1*$^{-/-}$ mice continued to show increased skin thickness measured by caliper (Figure 5E) and collagen content (Figure 5F) compared to WT mice after bleomycin treatment, but not after NaCl injections. We further confirmed the increased dermal thickness in *Lair1*$^{-/-}$ mice challenged with bleomycin by performing histology with Masson's trichrome staining (Figure 5G-H). By immunohistochemistry (IHC), we found an accompanying increase in αSMA+ dermal myofibroblasts (Figure 5I).

The increased fibrotic response in this model in *Lair1*$^{-/-}$ mice supports a non-redundant role of LAIR-1 in tissue repair and regulation of fibrosis. Absence of proper LAIR-1 ligation due to collagen degradation in fibrotic tissue could thus lead to continued propagation of the tissue repair response in diseases such as SSc.

Discussion

In this study, we show that LAIR-1 represents an essential control mechanism for tissue repair. This regulatory function can be obstructed by the production of decoy ligands in fibrotic tissue, potentially perpetuating the fibrotic process in diseases like SSc.

LAIR-1 expression and intrinsic function was comparable in cells from SSc patients and HC, which is in line with our previous findings, that under inflammatory conditions LAIR-1 is expressed and upon ligation still efficiently reduces cytokine production (Carvalheiro *et al.*, 2020). In addition, the concentration of soluble LAIR-1 antagonists in the circulation of SSc patients is similar to HC, in contrast to the increased concentration of sLAIR-1 and LAIR-2 observed in rheumatoid arthritis patients and in patients with autoimmune thyroid diseases (Olde Nordkamp et al., 2011; Simone et al., 2013).

Despite normal LAIR-1 expression and function in cells from SSc patients, an inadequate ligand might undermine its inhibitory function. Collagen synthesis is highly upregulated in SSc tissues, leading to compensatory collagen degradation mechanisms. Several MMPs, including MMP7, MMP9 and MMP12, are increased in SSc patients (Manetti et al., 2012; Peng et al., 2012), translating to increased concentrations of collagen degradation products in the circulation and in the skin, suggesting a high collagen turnover in this disease (Dobrota et al., 2021; Hunzelmann et al., 1998; Juhl et al., 2020). However, despite increased collagen degradation, excessive collagen production still results in an imbalance and enormous accumulation of collagen in tissues and organs of these patients (Dobrota *et al.*, 2021; Juhl *et al.*, 2020; Manetti *et al.*, 2012; Scheja et al., 2000).

We now report that even though LAIR-1 is able to bind to the fibrotic skin of SSc patients and to the ECM deposited by fibroblasts under pro-fibrotic conditions, it cannot be functionally activated by the collagen products that are formed. Thus, these structures may act as decoy ligands and compete with intact collagen to prevent inhibitory signaling by LAIR-1. We have previously described that LAIR-1 binding to trimeric collagen peptides is influenced by glycine-proline-hydroxyproline (GPO) content of collagen, although other factors contribute to the interaction as well (Lebbink *et al.*, 2006; Lebbink *et al.*, 2009). In addition, we identified a collagen peptide (II-17) that binds to LAIR-1 but is unable to induce LAIR-1 signaling (Lebbink

et al., 2009). Thus, biochemical and structural alterations of collagen determine the LAIR-1 functional response.

The inadequate activation of LAIR-1 by fibrotic collagen could be partly explained by the lack receptor clustering in analogy to glycoprotein VI (GPVI). GPVI is a collagen activating receptor on platelets and the collagen-binding domain is homologous of LAIR-1 (Brondijk et al., 2010; Jarvis et al., 2008; Lebbink *et al.*, 2009; Tomlinson et al., 2007). The proximity of GPVI dimer-binding sites on the collagen fiber surface enables clustering of GPVI dimers, increasing avidity and bringing together the necessary components to initiate receptor signaling (Herr and Farndale, 2009; Poulter et al., 2017). LAIR-1 may have similar requirements for signaling. While short collagen degradation products may be sufficient for LAIR-1 binding, signaling may require longer collagen fibers containing a greater number of binding sites for LAIR-1 clustering inducing a downstream signaling cascade.

The production of the fibrotic collagen products in our *in vitro* system upon repeated exposure to TGFβ and CXCL4 is dependent of PDGF receptor signaling and MMP activity. PDGF family members are potent mitogenic factors and are involved in chemotaxis and cell migration (Andrae *et al.*, 2008). Both PDGFs and PDGFRs are upregulated in skin lesions of SSc patients and this pathway promotes myofibroblast activation (Klinkhammer et al., 2018). In addition, PDGF proteins, particularly PDGF-D, upregulate the expression of multiple MMPs (Cui et al., 2014; Qin et al., 2016), and are consequently implicated in collagen degradation (Canalis et al., 1989). Collagen fragments, particularly 3/4 length collagen fragments, in turn enhance PDGF migratory properties (Stringa et al., 2000), which may contribute to the increased motility we observed upon TGFβ plus CXCL4 stimulation. Indeed, MMP inhibition reduced cell motility, in agreement with previous work (Li et al., 2004).

The presence of collagen degradation products in SSc may lead to an inefficient LAIR-1 inhibitory signal in immune cells and thus perpetuate inflammation and consequent fibrosis in these patients. In mice, LAIR-1 deficiency indeed resulted in increased bleomycin-induced skin fibrosis, also in response to repetitive injury promoted by saline injections. Absence of LAIR-1 resulted in an increased presence of αSMA^{+} myofibroblast and increased collagen deposition and dermal thickness. Thus, LAIR-1 deficient mice are more sensitive to developing fibrosis upon injury. This finding was consistent throughout experiments, although we did observe variability in the extension of the increased skin fibrosis in LAIR-1 deficient mice, reflected

either by skin caliper, collagen content or histology, which may have been due to differences in the efficacy of bleomycin inducing skin fibrosis as well as different operators performing the model in different experiments (Blyszczuk et al., 2019).

Since LAIR-1 is able to regulate a large variety of immune cells, it is possible that the exacerbated fibrotic phenotypic observed in LAIR-1 deficient mice is driven by multiple immune cells, including monocytes, macrophages, DCs, T cells and B cells. In particular, inflammatory monocytes and tissue-resident macrophages highly express LAIR-1 and are key regulators that maintain tissue homeostasis and are important for both driving and resolving tissue repair (Carvalheiro *et al.*, 2020; Keerthivasan *et al.*, 2021; Meizlish *et al.*, 2021). Further studies are needed to determine which cell types are essential for LAIR-1 mediated regulation of fibrosis.

Taken together, we identified a crucial role for LAIR-1 in the regulation of tissue repair using LAIR-1 deficient mice and show that in response to soluble factors that drive inflammation and fibrosis in SSc, human fibroblasts generate large amounts of degraded collagen, with impaired capacity to induce LAIR-1 signaling. Our data may explain how dysregulation can occur in fibrosis resulting in a vicious cycle: LAIR-1 normally senses collagen thus providing negative feedback to further collagen production, while collagen fragments, presumably generated during injury, prevent the negative feedback so that new collagen can be made to replace degraded collagen. However, fragments produced under inflammatory conditions can remove this negative feedback even when there is excess collagen present in fibrotic tissues. Thus, a circuit designed to maintain homeostasis has a vulnerability to dysregulation resulting in fibrosis.

Since LAIR-1 is expressed and intrinsically functional in SSc patients, our study opens novel avenues for the treatment of SSc and perhaps other fibrotic diseases by harnessing the LAIR-1 feedback loop to halt the cascade of inflammation and fibrosis.

Methods

Animal Experiments

Lair1$^{-/-}$ mice were generated on the C57BL/6 background by Taconic Artemis as described in (Smith et al., 2017). Female *Lair1*$^{-/-}$ and wild-type (WT) mice derived from the same breeding line and housed under the same conditions were used for this study. Animal experiments were approved by the Committee on Animal Experiments of the Utrecht University and performed at the Central Animal Laboratory, Utrecht University.

Bleomycin mouse model of SSc

WT and *Lair1*$^{-/-}$ female mice were treated daily with subcutaneous injections into the back during either 2 weeks (1 independent experiment, n=6 per group, age ±28 weeks,) or 4 weeks (1 independent experiment, n=6 per group, age ±12 weeks; 3 independent experiments, n=3-6 per group, age ±28 weeks) of bleomycin (200 µL, 1000 µg/mL or 500 µg/mL respectively, Bleomedac - Medac or Baxter). Two days after the last injections, mice were sacrificed by cervical dislocation.

Patients

Blood from SSc patients was obtained from the University Medical Center Utrecht and Maasstad Hospital Rotterdam. Early SSc (eaSSc) patients were classified according to Leroy and Medsger (LeRoy and Medsger, 2001). Definite SSc patients fulfilling the classification the American College of Rheumatology/European League Against Rheumatism 2013 classification criteria (van den Hoogen et al., 2013) without manifesting skin fibrosis were defined as non-cutaneous SSc (ncSSc); fibrotic SSc patients were stratified to limited cutaneous (lcSSc) or diffuse cutaneous SSc (dcSSc) according to the extent of skin involvement (LeRoy et al., 1988) (Supplementary table 1). Blood from sex- and age-matched healthy controls (HC) was obtained from the Mini Donor Service of the University Medical Center Utrecht. The study was conducted according to the Helsinki declaration and it was approved by the local institutional medical ethics review boards. All subjects provided written informed consent. Samples and clinical information were treated anonymously immediately after collection.

Histochemical Analysis

Skin sections (5 µm) of paraffin-embedded tissue were stained with Mason's trichrome, to evaluate collagen content and organization. For αSMA staining, deparaffinized sections were rehydrated, and streptavidin/biotin blocking kit (Vector Laboratories) was applied, followed by blocking step with normal goat serum (Cell Signaling Technology). Next, samples were stained with rabbit-anti mouse αSMA (2 µg/ml, Abcam); followed by a goat-anti rabbit antibody-biotin (1:300, Vector Laboratories) and subsequent Vectastain ABC HRP kit (Vector Laboratories). ImmPact NovaRED (Vector Laboratories) was used as substrate. Samples were counterstained with Mayer's hematoxylin. Images were acquired on an Aperio Digital Pathology Slide Scanner (Leica Biosytems). Images were analysed using the Aperio ImageScope software (Leica Biosytems) and dermal thickness was measured according to the protocol described by Błyszczuk *et al*. (Blyszczuk *et al.*, 2019).

Quantification of Tissue Collagen

Collagen content was quantified by colorimetric assays from 4 mm skin punch biopsies. Skin sections were hydrolyzed and collagen content was determined in supernatants by QuickZyme total collagen assay (QuickZyme Bioscience) or the Total Collagen Assay Kit (Abcam), according to the manufacturer's instructions.

Cell isolation

Peripheral blood was obtained from HC and SSc patients in lithium heparin tubes. Peripheral blood mononuclear cells (PBMCs) were isolated by density centrifugation using Ficoll-Paque Plus (GE Healthcare). Plasmacytoid dendritic cells and monocytes were isolated using anti-BDCA4 or anti-CD14 magnetic microbeads (Miltenyi Biotec) respectively, based on positive separation on auto-MACS assisted cell sorting (Miltenyi Biotec) according to the manufacturer's protocol.

Flow cytometry analysis

LAIR-1 expression on PBMCs was determined on freshly isolated cells, blocked with normal mouse serum (Fitzgerald) and then stained for 20 min at 4°C with fluorochome-conjugated monoclonal antibodies according to the panel on Supplementary table 2. Samples were acquired on a BD LSR Fortessa (BD Biosciences) using the BD FACSDiva software (BD

Biosciences). FlowJo software (Tree Star) was used for data analyses (analysis strategy in Supplemental Figure 6A-B).

Immunohistochemistry staining for LAIR-1

Skin frozen sections (6 µm) from HC and SSc patients samples were fixed in 10% neutral buffered formalin for 15 sec. at room temperature (RT). After washing step with PBS+0.05% Tween-20, 0.3% Hydrogen peroxide was applied to the specimens, that were then blocked with 2.5% normal horse serum (Vector Laboratories) diluted in PBS. Next, 10 µg/mL of either mouse anti-human LAIR-1 (clone Dx26; purified in house) or mouse isotype control IgG1 (Dako) diluted in PBS+1% BSA buffer were incubated overnight at 4°C. Samples were then washed and incubated for 30 min with anti –mouse Ig HPR (Vector Laboratories). After washing, AEC+ Substrate-Chromogen (Dako) was used as substrate. Samples were counterstained with Mayer's hematoxylin. Image acquisition was performed on an Olympus BX41 microscope. Images were further processed with ImageJ software. A representative LAIR-1 and isotype control staining is shown in Supplemental Figure 7A.

Analysis of LAIR-1 function

LAIR-1 inhibitory function was assessed on purified pDCs and purified monocytes from HC and SSc patients as described before (Carvalheiro *et al.*, 2020). Briefly, 96 well Nunc culture or 24 well Nunc culture plates (Thermo Fisher Scientific) were coated with 10 µg/mL of anti-LAIR-1 agonist mAb (clone Dx26) or 10 µg/mL of mouse isotype control IgG1 (eBioscience- Thermo Fisher Scientific) diluted in PBS overnight at 4°C. A total of $5.0x10^4$ pDCs or $5.0x10^5$ monocytes were seeded in the pre-coated plates with RPMI 1640 GlutaMAX (Life Technologies- Thermo Fisher Scientific), supplemented with 10% heat-inactivated fetal calf serum (FCS, Biowest Riverside) and 1% penicillin/streptomycin (Thermo Fisher Scientific), after incubation with Fc receptor blocking reagent (Miltenyi Biotech), for 2 hours at 37°C in a 5% CO_2 incubator. Then, pDCs were either left unstimulated or stimulated with CPG-C-TLR9 ligand (500 µM) and monocytes were either left unstimulated or stimulated with LPS-TLR4 ligand (100 ng/mL), all from Invivogen. Cells were incubated overnight at 37°C in a 5% CO_2 incubator and afterwards supernatants were harvested and stored at -80°C until further analysis.

Measurement of cytokine production

Cytokines in cell-free supernatants were measured using enzyme-linked immunosorbent assay (ELISA) for IL-6 (Sanquin), TNF-α (Diaclone) and IFN-α (eBiosience, Thermo Fisher Scientific), following the manufacturer's instructions. The cytokine production in monocytes and pDCs from HC and SSc patients upon stimulation is shown in Supplementary table 3. Soluble (s)LAIR-1 (as described previously (Olde Nordkamp *et al.*, 2011)) and LAIR-2 (LifeSpan BioSciences) were also measured by ELISA in the serum of HC and SSc patients.

LAIR-1 - Collagen binding assay

Collagen binding to LAIR-1 stably transduced K562-cells (Lebbink *et al.*, 2006) was assessed by flow cytometry adapted from the previously described protocol (Lenting et al., 2010). In brief, collagen I FITC labelled was incubated for 1 hour at room temperature with serum either from SSc patients or HC (1:30 dilution). Next, $1.5x10^5$ K562-cells overexpressing LAIR-1 were incubated with the collagen-serum mix during 30 min. After a washing step, cells were incubated with anti-LAIR-1 PE (clone Dx26, BD) for 15 min and then washed. Samples were acquired on a BD LSR Fortessa (BD Biosciences) using the BD FACSDiva software (BD Biosciences). The percentage (%) of cells binding to collagen was determined using the FlowJo software (Tree Star).

Human skin staining with hLAIR-1-IgG

Frozen tissue sections (5 µm) from SSc and HC skin that were fixed in 10% acetone in the presence of 1.5% H_2O_2. Free biotin in the sections was blocked using the streptavidin/biotin blocking kit (Vector Laboratories). Tissue sections were stained with biotinylated hLAIR-1–IgG (a chimeric protein obtained by fusing the extracellular domain of human(h)LAIR-1 to the Fc region of human IgG1 (Lebbink et al., 2004)), in the presence of 2% FCS. After washing with PBS, sections were treated with streptABComplex/HRP (Vector Laboratories) according to the manufacturer's instructions, followed by AEC+ substrate-chromogen (Dako) and counterstained with hematoxylin. Images were acquired on an Olympus BX41 microscope and to quantify the hLAIR1-IgG staining, HALO (Indica Labs) Area Quantification-v1 algorithm was used with thresholds for positive and negative signals set based on controls. A classifier was built to identify the dermis, and used within the analysis algorithm to quantify IHC signal and reduce the background from pigmented skin samples.

Dermal fibroblasts culture

Dermal fibroblasts were isolated from 3–4-mm skin biopsy sections obtained from a clinically affected area of SSc patients, while HC dermal fibroblasts were obtained from skin biopsy sections as resected material after cosmetic surgery. Dermal fibroblast isolation was performed using a whole skin dissociation kit (Miltenyi Biotec) following the manufacturer's instructions, and fibroblasts were routinely maintained in Dulbecco's modified Eagle's medium (DMEM; Invitrogen) supplemented with 10% FBS and 1% penicillin–streptomycin. Cells were used for experiments between passages 3 and 5.

In vitro fibrotic model

Nunc Lab-Tek II chamber slides (ThermoFisher Scientific) or µ-Slide 8 Well Glass Bottom (IBIDI) were precoated with 0.001% poly-l-lysine (Sigma-Aldrich), washed with PBS and air-dried. Dermal fibroblasts were seeded in DMEM containing 10% FBS for 24 hours and then incubated overnight in DMEM containing 0.1% FBS. Cells were then stimulated with recombinant TGFβ2 (10 ng/mL, R&D Systems), recombinant CXCL4 (5 µg/mL, Peprotech) or the combination of both in DMEM containing 2% FBS and 50 µg/ml of L-ascorbic acid (Wako Pure Chemical), and refreshed 2 and 4 days later. Where indicated, PDGFR inhibitor CP-868596/Crenolanib (Selleckchem) and the metalloproteinase inhibitor GM6001/ Galardin (Merck Millipore) were used at the concentration of 1 µM and 100 µM respectively and refreshed as described above. In some experiments cells under stimulation were imaged live on the IncuCyte system (Essen BioScience). After 6 days of stimulation, or otherwise indicated, cells were used for immunofluorescence, electron microscopy analysis or reporter cell assay.

Immunofluorescence

Cells were fixed with 4% paraformaldehyde, washed with PBS–1% bovine serum albumin (BSA), and blocked in PBS containing 5% normal serum and 1% BSA. Cells were incubated with biotinylated hLAIR-1-IgG, anti-collagen I, or pan-anti-collagen antibody mix (anti-collagen I, II, III, IV, V) for 1 hour at room temperature, washed, and incubated with secondary antibodies conjugated with Alexa Fluor 488, Alexa Fluor 594 or Alexa Fluor 647 for 30 minutes at room temperature (Supplementary table 2 for antibody information).

The collagen hybridizing peptide (CHP, 3Helix) staining was performed according to the manufacturer’s protocol. Briefly, cells were fixed with 4% paraformaldehyde and washed with

PBS+1% BSA. Next, samples were blocked with 5% normal goat serum and 1% BSA and then incubated for 2 hours at 4°C with biotinylated CHP (2.5 µM), previously denatured at 80°C for 5 min (non-denatured CHP was used to assess unspecific binding) plus LAIR-1-IgG (5 µg/mL). After washing with PBS+1% BSA, samples were incubated 1 hour at room temperature with unlabeled anti-LAIR-1 mAb (2.5 µg/mL, clone Dx26) followed by a last step incubation with streptavidin AF647 and goat anti-mouse AF488 (both 2 µg/mL).

Cells were incubated with DAPI (Sigma-Aldrich) for 15 min at room temperature and finally washed with PBS.

Imaging data were acquired on a Zen2009 LSM 710 confocal microscope (Zeiss) or on the IncuCyte system (Essen BioScience). For the quantification of LAIR-1-IgG and Collagen I co-staining the .lsm files were converted to .czi files and then analyzed using HALO (Indica Labs) Area Quantification FL v1 algorithm. Positive and negative samples were used to set thresholds for each marker. To quantify the areas of plaques (hLAIR-1-IgG binding structures), HALO classifiers were trained on negative and positive samples. Separate classifiers were developed for images captured on the Incucyte versus the Zen2009 LSM 710 confocal microscope.

Electron microscopy

Dermal fibroblasts were grown on carbon coated glass coverslips as described above, fixed with 4% Formaldehyde, labelled with pan-collagen mix of antibodies antibody, hLAIR-1-IgG fusion protein, and counterstained with DAPI as also stated above. The coverslips were imaged in the fluorescence microscope (Thunder, Leica) to confirm the presence of LAIR-1 binding ECM structures. After fluorescence microscopy, cells on coverslips were fixed in half strength Karnovsky fixative (2.5% Glutaraldehyde (EMS) + 2% Formaldehyde (Sigma)) pH 7.4 at RT for 2 h. Cells were rinsed and stored in 1M Phoshate Buffer pH 7.4 at 4°C until further processing. Post-fixation was performed with 1% OsO4, 1.5% K3Fe(III)(CN)6 in 1M Phoshate Buffer pH 7.4 for 2 h. Cells were then dehydrated in a series of aceton, and flat embedded in Epon (SERVA) similar to reported before (Fermie et al., 2018). After curing, the coverslips were detached from the resin block and ultrathin sections were cut (Leica Ultracut UCT), collected on formvar and carbon coated transmission electron microscopy (TEM) grids, and stained with uranyl acetate and lead citrate (Leica AC20). Micrographs were collected on a JEM1010 (JEOL) equipped with

a Veleta 2k×2k CCD camera (EMSIS, Munster, Germany) or on a Tecnai12 (FEI Thermo Fisher) equipped with a Veleta 2k×2k CCD camera (EMSIS, Munster, Germany) and operating SerialEM software.

Binding assay

96-well black flat-bottom plates (Corning) were coated overnight at 4 °C with purified collagen I from human placenta (Sigma), gelatin from bovine skin (Sigma) or BSA (for unspecific binding) diluted in PBS (50 µL/well). After washing with PBS, proteins were fixed with 100% ice-cold methanol at -20°C for 30 min and then washed. Wells were then blocked for 30 min with PBS containing 1% of normal donkey serum and 2% FBS. Blocking solution was discarded and replaced with hLAIR-1-IgG biotinylated (5 µg/mL) and incubated for 1 hour at RT. After washing, wells were incubated with a Streptavidin AF647 (5 µg/mL) for 1 hour at RT. After washing, imaging and data acquisition was performed on a LI-COR - Odyssey system. Signal intensity was obtained for each well.

Reporter cell assay

2B4 T cell hybridoma cells with stable expression of a NFAT-GFP reporter and hLAIR-1-CD3ζ or WT-CD3ζ were cultured as previously described (Lebbink *et al.*, 2006). To assess hLAIR-1-CD3ζ response to either purified collagen I or gelatin, 96-well black flat-bottom plates (Corning) were coated overnight at 4 °C with purified collagen I from human placenta (Sigma), gelatin from bovine skin (Sigma) or BSA (for unspecific binding) diluted in PBS (50 µL/well). After washings, 5.0×10^4 cells in 200 µL were added to each well, and plates were incubated at 37°C for 20 h and analyzed for GFP expression by flow cytometry.

To evaluate hLAIR-1-CD3ζ response to fibrotic ECM, dermal fibroblasts cultured and stimulated as described above, were rinsed with PBS and $1.5\text{x}10^5$ hLAIR-1-CD3ζ - NFAT-GFP reporter cells were added. For the experiment controls, µ-Slide 8 Well Glass Bottom (IBIDI) were coated overnight at 4°C with purified collagen I, BSA, or anti–hLAIR-1 mAb (clone Dx26) at 5 µg/mL in PBS. After washing, cells were added to each well. Cells were incubated for 20 hours and GFP expression was measured by flow cytometry. In parallel, samples were incubated in the IncuCyte system and live imaging was performed during 70 hours to determine GFP expression. Efficiency of the LAIR-1-CD3ζ and WT- CD3ζ response are shown in Supplemental Figure 8.

LAIR-1 expression from profiling data

LAIR-1 gene expression was retrieved from array profiling data available on the Gene Expression Omnibus (GEO – NCBI) using GEO2R (NCBI).

Statistics

Statistical analysis was performed using GraphPad Prism 8 software (GraphPad Software Inc.). Differences between experimental groups were analyzed using parametric paired t-tests, one-way ANOVA test or non-parametric Mann–Whitney U test or Wilcoxon's test, when appropriate. Pearson's correlation coefficient test was applied to detect the association between different parameters. Two-sided testing was performed for all analyses. Differences were considered to be statistically significant at $p<0.05$

Author contributions:

TC, WM, TRDJR and LM were involved in study conception. TC, WM, SG, MIP, JK, NL, TRDJR and LM designed the experimental approach and interpreted the data. TC, WM, SG, MIP, AJA, ASM, BG, RGT, EE, MLM and TV carried out the experiments. TC, DF, TV and LV performed data analysis. AO and MC collected and supplied clinical data. MR and MEMG reviewed data. TC and LM wrote the original draft. All authors critically revised the manuscript and approved the final version.

Acknowledgements

TC was supported by a grant from the Portuguese national funding agency for science, research, and technology: Fundação para a Ciência e a Tecnologia [SFRH/BD/93526/2013]. S.G. is supported by the Miguel Servet program (CP19/00005) from the Instituto de Salud Carlos III (ISCIII) and the European Social Fund ("Investing in your future"). LM is supported by the Dutch Research Council (NWO) (Vici 918.15.608). The electron microscopy within this work is part of the research program National Roadmap for Large-Scale Research Infrastructure (NEMI), financed by NWO (184.034.014) to JK. NL is financed by ZonMw TOP grant (40-00812-98-16006) to JK and Anna Akhmanova. Part of this study was supported by an investigator-initiated collaborative research agreement between University Medical Centre Utrecht and Boehringer Ingelheim.

We would like to thank to Department of Rheumatology & Clinical Immunology in University Medical Centre Utrecht and to the Department of Rheumatology and Clinical Immunology, Maasstad Hospital Rotterdam for patient inclusion. We would also like to thank Karin de Cortie (University Medical Center Utrecht) for the technical support with the animal experiments.

Graphical abstract was created with BioRender.com.

Conflict of Interest

DF, MR and MEMG are full time employees of Boehringer Ingelheim. The remaining authors declare that the research was conducted in the absence of any commercial or financial relationships that could be construed as a potential conflict of interest.

References

Allanore, Y., Simms, R., Distler, O., Trojanowska, M., Pope, J., Denton, C.P., and Varga, J. (2015). Systemic sclerosis. Nat Rev Dis Primers *1*, 15002. 10.1038/nrdp.2015.2.

Andrae, J., Gallini, R., and Betsholtz, C. (2008). Role of platelet-derived growth factors in physiology and medicine. Genes Dev *22*, 1276-1312. 10.1101/gad.1653708.

Blyszczuk, P., Kozlova, A., Guo, Z., Kania, G., and Distler, O. (2019). Experimental Mouse Model of Bleomycin-Induced Skin Fibrosis. Curr Protoc Immunol *126*, e88. 10.1002/cpim.88.

Bonaccorsi, I., Cantoni, C., Carrega, P., Oliveri, D., Lui, G., Conte, R., Navarra, M., Cavaliere, R., Traggiai, E., Gattorno, M., et al. (2010). The immune inhibitory receptor LAIR-1 is highly expressed by plasmacytoid dendritic cells and acts complementary with NKp44 to control IFNalpha production. PLoS One *5*, e15080. 10.1371/journal.pone.0015080.

Brondijk, T.H., de Ruiter, T., Ballering, J., Wienk, H., Lebbink, R.J., van Ingen, H., Boelens, R., Farndale, R.W., Meyaard, L., and Huizinga, E.G. (2010). Crystal structure and collagen-binding site of immune inhibitory receptor LAIR-1: unexpected implications for collagen binding by platelet receptor GPVI. Blood *115*, 1364-1373. 10.1182/blood-2009-10-246322.

Canalis, E., McCarthy, T.L., and Centrella, M. (1989). Effects of platelet-derived growth factor on bone formation in vitro. J Cell Physiol *140*, 530-537. 10.1002/jcp.1041400319.

Carvalheiro, T., Garcia, S., Pascoal Ramos, M.I., Giovannone, B., Radstake, T., Marut, W., and Meyaard, L. (2020). Leukocyte Associated Immunoglobulin Like Receptor 1 Regulation and Function on Monocytes and Dendritic Cells During Inflammation. Front Immunol *11*, 1793. 10.3389/fimmu.2020.01793.

Cui, Y., Sun, Y.W., Lin, H.S., Su, W.M., Fang, Y., Zhao, Y., Wei, X.Q., Qin, Y.H., Kohama, K., and Gao, Y. (2014). Platelet-derived growth factor-BB induces matrix metalloproteinase-2 expression and rat vascular smooth muscle cell migration via ROCK and ERK/p38 MAPK pathways. Mol Cell Biochem *393*, 255-263. 10.1007/s11010-014-2068-5.

Denton, C.P., and Khanna, D. (2017). Systemic sclerosis. Lancet *390*, 1685-1699. 10.1016/S0140-6736(17)30933-9.

Distler, J.H.W., Gyorfi, A.H., Ramanujam, M., Whitfield, M.L., Konigshoff, M., and Lafyatis, R. (2019). Shared and distinct mechanisms of fibrosis. Nat Rev Rheumatol *15*, 705-730. 10.1038/s41584-019-0322-7.

Dobrota, R., Jordan, S., Juhl, P., Maurer, B., Wildi, L., Bay-Jensen, A.C., Karsdal, M.A., Herrick, A.L., Distler, J.H.W., Allanore, Y., et al. (2021). Circulating collagen neo-epitopes and their role in the prediction of fibrosis in patients with systemic sclerosis: a multicentre cohort study. Lancet Rheumatol *3*, E175-E184. 10.1016/S2665-9913(20)30385-4.

Fermie, J., Liv, N., Ten Brink, C., van Donselaar, E.G., Muller, W.H., Schieber, N.L., Schwab, Y., Gerritsen, H.C., and Klumperman, J. (2018). Single organelle dynamics linked to 3D structure by correlative live-cell imaging and 3D electron microscopy. Traffic *19*, 354-369. 10.1111/tra.12557.

Henderson, N.C., Rieder, F., and Wynn, T.A. (2020). Fibrosis: from mechanisms to medicines. Nature *587*, 555-566. 10.1038/s41586-020-2938-9.

Herr, A.B., and Farndale, R.W. (2009). Structural insights into the interactions between platelet receptors and fibrillar collagen. J Biol Chem *284*, 19781-19785. 10.1074/jbc.R109.013219.

Hunzelmann, N., Risteli, J., Risteli, L., Sacher, C., Vancheeswaran, R., Black, C., and Krieg, T. (1998). Circulating type I collagen degradation products: a new serum marker for clinical severity in patients with scleroderma? Br J Dermatol *139*, 1020-1025. 10.1046/j.1365-2133.1998.02558.x.

Hwang, J., Huang, Y., Burwell, T.J., Peterson, N.C., Connor, J., Weiss, S.J., Yu, S.M., and Li, Y. (2017). In Situ Imaging of Tissue Remodeling with Collagen Hybridizing Peptides. ACS Nano *11*, 9825-9835. 10.1021/acsnano.7b03150.

Jansen, C.A., Cruijsen, C.W., de Ruiter, T., Nanlohy, N., Willems, N., Janssens-Korpela, P.L., and Meyaard, L. (2007). Regulated expression of the inhibitory receptor LAIR-1 on human peripheral T cells during T cell activation and differentiation. Eur J Immunol *37*, 914-924. 10.1002/eji.200636678.

Jarvis, G.E., Raynal, N., Langford, J.P., Onley, D.J., Andrews, A., Smethurst, P.A., and Farndale, R.W. (2008). Identification of a major GpVI-binding locus in human type III collagen. Blood *111*, 4986-4996. 10.1182/blood-2007-08-108472.

Juhl, P., Bay-Jensen, A.C., Hesselstrand, R., Siebuhr, A.S., and Wuttge, D.M. (2020). Type III, IV, and VI Collagens Turnover in Systemic Sclerosis - a Longitudinal Study. Sci Rep *10*, 7145. 10.1038/s41598-020-64233-8.

Kania, G., Rudnik, M., and Distler, O. (2019). Involvement of the myeloid cell compartment in fibrogenesis and systemic sclerosis. Nat Rev Rheumatol *15*, 288-302. 10.1038/s41584-019-0212-z.

Karsdal, M.A., Nielsen, S.H., Leeming, D.J., Langholm, L.L., Nielsen, M.J., Manon-Jensen, T., Siebuhr, A., Gudmann, N.S., Ronnow, S., Sand, J.M., et al. (2017). The good and the bad collagens of fibrosis - Their role in signaling and organ function. Adv Drug Deliv Rev *121*, 43-56. 10.1016/j.addr.2017.07.014.

Keerthivasan, S., Senbabaoglu, Y., Martinez-Martin, N., Husain, B., Verschueren, E., Wong, A., Yang, Y.A., Sun, Y., Pham, V., Hinkle, T., et al. (2021). Homeostatic functions of monocytes and interstitial lung macrophages are regulated via collagen domain-binding receptor LAIR1. Immunity *54*, 1511-1526 e1518. 10.1016/j.immuni.2021.06.012.

Klinkhammer, B.M., Floege, J., and Boor, P. (2018). PDGF in organ fibrosis. Mol Aspects Med *62*, 44-62. 10.1016/j.mam.2017.11.008.

Lebbink, R.J., de Ruiter, T., Adelmeijer, J., Brenkman, A.B., van Helvoort, J.M., Koch, M., Farndale, R.W., Lisman, T., Sonnenberg, A., Lenting, P.J., and Meyaard, L. (2006). Collagens are functional, high affinity ligands for the inhibitory immune receptor LAIR-1. J Exp Med *203*, 1419-1425. 10.1084/jem.20052554.

Lebbink, R.J., de Ruiter, T., Verbrugge, A., Bril, W.S., and Meyaard, L. (2004). The mouse homologue of the leukocyte-associated Ig-like receptor-1 is an inhibitory receptor that recruits Src homology region 2-containing protein tyrosine phosphatase (SHP)-2, but not SHP-1. J Immunol *172*, 5535-5543. 10.4049/jimmunol.172.9.5535.

Lebbink, R.J., Raynal, N., de Ruiter, T., Bihan, D.G., Farndale, R.W., and Meyaard, L. (2009). Identification of multiple potent binding sites for human leukocyte associated Ig-like receptor LAIR on collagens II and III. Matrix Biol *28*, 202-210. 10.1016/j.matbio.2009.03.005.

Lebbink, R.J., van den Berg, M.C., de Ruiter, T., Raynal, N., van Roon, J.A., Lenting, P.J., Jin, B., and Meyaard, L. (2008). The soluble leukocyte-associated Ig-like receptor (LAIR)-2 antagonizes

the collagen/LAIR-1 inhibitory immune interaction. J Immunol *180*, 1662-1669. 10.4049/jimmunol.180.3.1662.

Lenting, P.J., Westerlaken, G.H., Denis, C.V., Akkerman, J.W., and Meyaard, L. (2010). Efficient inhibition of collagen-induced platelet activation and adhesion by LAIR-2, a soluble Ig-like receptor family member. PLoS One *5*, e12174. 10.1371/journal.pone.0012174.

LeRoy, E.C., Black, C., Fleischmajer, R., Jablonska, S., Krieg, T., Medsger, T.A., Jr., Rowell, N., and Wollheim, F. (1988). Scleroderma (systemic sclerosis): classification, subsets and pathogenesis. J Rheumatol *15*, 202-205.

LeRoy, E.C., and Medsger, T.A., Jr. (2001). Criteria for the classification of early systemic sclerosis. J Rheumatol *28*, 1573-1576.

Li, W., Fan, J., Chen, M., Guan, S., Sawcer, D., Bokoch, G.M., and Woodley, D.T. (2004). Mechanism of human dermal fibroblast migration driven by type I collagen and platelet-derived growth factor-BB. Mol Biol Cell *15*, 294-309. 10.1091/mbc.e03-05-0352.

Lodyga, M., and Hinz, B. (2020). TGF-beta1 - A truly transforming growth factor in fibrosis and immunity. Semin Cell Dev Biol *101*, 123-139. 10.1016/j.semcdb.2019.12.010.

Lu, P., Takai, K., Weaver, V.M., and Werb, Z. (2011). Extracellular matrix degradation and remodeling in development and disease. Cold Spring Harb Perspect Biol *3*. 10.1101/cshperspect.a005058.

Maasho, K., Masilamani, M., Valas, R., Basu, S., Coligan, J.E., and Borrego, F. (2005). The inhibitory leukocyte-associated Ig-like receptor-1 (LAIR-1) is expressed at high levels by human naive T cells and inhibits TCR mediated activation. Mol Immunol *42*, 1521-1530. 10.1016/j.molimm.2005.01.004.

Manetti, M., Guiducci, S., Romano, E., Bellando-Randone, S., Conforti, M.L., Ibba-Manneschi, L., and Matucci-Cerinic, M. (2012). Increased serum levels and tissue expression of matrix metalloproteinase-12 in patients with systemic sclerosis: correlation with severity of skin and pulmonary fibrosis and vascular damage. Ann Rheum Dis *71*, 1064-1072. 10.1136/annrheumdis-2011-200837.

Meizlish, M.L., Franklin, R.A., Zhou, X., and Medzhitov, R. (2021). Tissue Homeostasis and Inflammation. Annu Rev Immunol *39*, 557-581. 10.1146/annurev-immunol-061020-053734.

Merlo, A., Tenca, C., Fais, F., Battini, L., Ciccone, E., Grossi, C.E., and Saverino, D. (2005). Inhibitory receptors CD85j, LAIR-1, and CD152 down-regulate immunoglobulin and cytokine production by human B lymphocytes. Clin Diagn Lab Immunol *12*, 705-712. 10.1128/CDLI.12.6.705-712.2005.

Meyaard, L., Adema, G.J., Chang, C., Woollatt, E., Sutherland, G.R., Lanier, L.L., and Phillips, J.H. (1997). LAIR-1, a novel inhibitory receptor expressed on human mononuclear leukocytes. Immunity *7*, 283-290.

Okabe, Y., and Medzhitov, R. (2016). Tissue biology perspective on macrophages. Nat Immunol *17*, 9-17. 10.1038/ni.3320.

Olde Nordkamp, M.J., van Roon, J.A., Douwes, M., de Ruiter, T., Urbanus, R.T., and Meyaard, L. (2011). Enhanced secretion of leukocyte-associated immunoglobulin-like receptor 2 (LAIR-2) and soluble LAIR-1 in rheumatoid arthritis: LAIR-2 is a more efficient antagonist of the LAIR-1-collagen inhibitory interaction than is soluble LAIR-1. Arthritis Rheum *63*, 3749-3757. 10.1002/art.30612.

Park, J.E., Brand, D.D., Rosloniec, E.F., Yi, A.K., Stuart, J.M., Kang, A.H., and Myers, L.K. (2020). Leukocyte-associated immunoglobulin-like receptor 1 inhibits T-cell signaling by decreasing protein phosphorylation in the T-cell signaling pathway. J Biol Chem *295*, 2239-2247. 10.1074/jbc.RA119.011150.

Peng, W.J., Yan, J.W., Wan, Y.N., Wang, B.X., Tao, J.H., Yang, G.J., Pan, H.F., and Wang, J. (2012). Matrix metalloproteinases: a review of their structure and role in systemic sclerosis. J Clin Immunol *32*, 1409-1414. 10.1007/s10875-012-9735-7.

Poulter, N.S., Pollitt, A.Y., Owen, D.M., Gardiner, E.E., Andrews, R.K., Shimizu, H., Ishikawa, D., Bihan, D., Farndale, R.W., Moroi, M., et al. (2017). Clustering of glycoprotein VI (GPVI) dimers upon adhesion to collagen as a mechanism to regulate GPVI signaling in platelets. J Thromb Haemost *15*, 549-564. 10.1111/jth.13613.

Qin, Z., Feng, J., Liu, Y., Deng, L.L., and Lu, C. (2016). PDGF-D promotes dermal fibroblast invasion in 3-dimensional extracellular matrix via Snail-mediated MT1-MMP upregulation. Tumour Biol *37*, 591-599. 10.1007/s13277-015-3828-x.

Rockey, D.C., Bell, P.D., and Hill, J.A. (2015). Fibrosis--a common pathway to organ injury and failure. N Engl J Med *372*, 1138-1149. 10.1056/NEJMra1300575.

Scheja, A., Wildt, M., Wollheim, F.A., Akesson, A., and Saxne, T. (2000). Circulating collagen metabolites in systemic sclerosis. Differences between limited and diffuse form and relationship with pulmonary involvement. Rheumatology (Oxford) *39*, 1110-1113. 10.1093/rheumatology/39.10.1110.

Simone, R., Pesce, G., Antola, P., Merlo, D.F., Bagnasco, M., and Saverino, D. (2013). Serum LAIR-2 is increased in autoimmune thyroid diseases. PLoS One *8*, e63282. 10.1371/journal.pone.0063282.

Smith, C.W., Thomas, S.G., Raslan, Z., Patel, P., Byrne, M., Lordkipanidze, M., Bem, D., Meyaard, L., Senis, Y.A., Watson, S.P., and Mazharian, A. (2017). Mice Lacking the Inhibitory Collagen Receptor LAIR-1 Exhibit a Mild Thrombocytosis and Hyperactive Platelets. Arterioscler Thromb Vasc Biol *37*, 823-835. 10.1161/ATVBAHA.117.309253.

Son, M., and Diamond, B. (2015). C1q-mediated repression of human monocytes is regulated by leukocyte-associated Ig-like receptor 1 (LAIR-1). Mol Med *20*, 559-568. 10.2119/molmed.2014.00185.

Son, M., Santiago-Schwarz, F., Al-Abed, Y., and Diamond, B. (2012). C1q limits dendritic cell differentiation and activation by engaging LAIR-1. Proc Natl Acad Sci U S A *109*, E3160-3167. 10.1073/pnas.1212753109.

Stringa, E., Knauper, V., Murphy, G., and Gavrilovic, J. (2000). Collagen degradation and platelet-derived growth factor stimulate the migration of vascular smooth muscle cells. J Cell Sci *113 (Pt 11)*, 2055-2064.

Theocharis, A.D., Skandalis, S.S., Gialeli, C., and Karamanos, N.K. (2016). Extracellular matrix structure. Adv Drug Deliv Rev *97*, 4-27. 10.1016/j.addr.2015.11.001.

Tomlinson, M.G., Calaminus, S.D., Berlanga, O., Auger, J.M., Bori-Sanz, T., Meyaard, L., and Watson, S.P. (2007). Collagen promotes sustained glycoprotein VI signaling in platelets and cell lines. J Thromb Haemost *5*, 2274-2283. 10.1111/j.1538-7836.2007.02746.x.

van Bon, L., Affandi, A.J., Broen, J., Christmann, R.B., Marijnissen, R.J., Stawski, L., Farina, G.A., Stifano, G., Mathes, A.L., Cossu, M., et al. (2014). Proteome-wide analysis and CXCL4 as a biomarker in systemic sclerosis. N Engl J Med *370*, 433-443. 10.1056/NEJMoa1114576.

van den Hoogen, F., Khanna, D., Fransen, J., Johnson, S.R., Baron, M., Tyndall, A., Matucci-Cerinic, M., Naden, R.P., Medsger, T.A., Jr., Carreira, P.E., et al. (2013). 2013 classification criteria for systemic sclerosis: an American College of Rheumatology/European League against Rheumatism collaborative initiative. Arthritis Rheum *65*, 2737-2747. 10.1002/art.38098.

Varga, J.A., and Trojanowska, M. (2008). Fibrosis in systemic sclerosis. Rheum Dis Clin North Am *34*, 115-143; vii. 10.1016/j.rdc.2007.11.002.

Weiskirchen, R., Weiskirchen, S., and Tacke, F. (2019). Organ and tissue fibrosis: Molecular signals, cellular mechanisms and translational implications. Mol Aspects Med *65*, 2-15. 10.1016/j.mam.2018.06.003.

Wynn, T.A. (2008). Cellular and molecular mechanisms of fibrosis. J Pathol *214*, 199-210. 10.1002/path.2277.

Yamamoto, T., Takagawa, S., Katayama, I., Yamazaki, K., Hamazaki, Y., Shinkai, H., and Nishioka, K. (1999). Animal model of sclerotic skin. I: Local injections of bleomycin induce sclerotic skin mimicking scleroderma. J Invest Dermatol *112*, 456-462. 10.1046/j.1523-1747.1999.00528.x.

Zeltz, C., and Gullberg, D. (2016). The integrin-collagen connection--a glue for tissue repair? J Cell Sci *129*, 653-664. 10.1242/jcs.180992.

Figure legends

Figure 1. LAIR-1 is expressed on circulating peripheral blood cells and in the skin of SSc patients and its intrinsic function is normal. (A) LAIR-1 expression on circulating immune cells (classical, intermediate and non-classical monocytes, cDC2, pDC, $CD4^+$ and $CD8^+$ T cells, $CD56^{bright}$ and $CD56^{dim}$ NK cells and B cells) from HC (n=14) and SSc patients (n=26) determined using flow cytometry. **(B)** Representative images of LAIR-1 expression (shown as red precipitate) in affected and non-affected skin from HC skin (n=3) and SSc patients (n=3), assessed by immunohistochemistry. **(C)** LAIR-1 function in monocytes and pDC from HC (n=6) and SSc patients (n=7). Isolated cells were pre-treated with a plate bound LAIR-1 agonist mAb (clone Dx26) or isotype control antibody. Monocytes were subsequently stimulated (24 hours) with LPS – TLR4 ligand, while pDCs were stimulated (24 hours) with CpC-C – TLR9 ligand. Production of IL-6 and TNF-α by monocytes and IFN-α by pDCs was determined by ELISA. Percentage (%) inhibition of cytokine production by LAIR-1 mAb is shown. **(D)** Effect of serum from HC and SSc patients to block LAIR-1 – collagen interaction. FITC labelled collagen was incubated either with sera from HC (n=20) or SSc patients (n=36) and the binding capacity of collagen to bind K562 cells overexpressing LAIR-1 was determined by flow cytometry. Collagen alone and blocking with recombinant LAIR-2 (40 µg/mL) are shown as controls with the dashed lines. Serum levels of **(E)** soluble LAIR-1 and **(F)** LAIR-2 in circulation of HC (n=10) and SSc patients (n=30) determined using ELISA. Results are represented as mean ± SD. Differences were considered statistically significant when $*p < 0.05$ (Mann–Whitney test).

Figure 2. LAIR 1 binds to *in vitro* and *in vivo* fibrotic ECM. (A) Representative immunohistochemistry staining and quantification of the hLAIR-1-IgG fusion protein (shown in red) and counterstained with hematoxylin in the skin of HC (n=9) and SSc patients (n=9). **(B)** Representative images of immunofluorescence (IF) staining with collagen I antibody (green), hLAIR-1-IgG fusion protein (red) and DAPI (blue) of ECM produced by dermal fibroblasts from HC (n=4) and SSc patients (n=4) stimulated with either medium, TGF-β2 or CXCL4. Quantification of % area with co-expression of Collagen I and hLAIR-1-IgG is shown. **(C)** Representative IF staining with collagen I antibody (green), hLAIR-1-IgG fusion protein (red) and DAPI (blue) of ECM produced by HC dermal fibroblasts stimulated with medium,

TGF-β2, CXCL4 or TGF-β2 combined with CXCL4. White arrows indicate deposits of LAIR-1 binding structures (representative of n=2). The area (μm^2) of hLAIR-1-IgG plaques is quantified **(D)** Representative IF staining with hLAIR-1-gG fusion protein (red), pan collagen antibodies (mix of collagen I, II, III, IV and V antibodies) (green) and DAPI (blue) of ECM produced by HC dermal fibroblasts stimulated with medium, TGF-β2, CXCL4 or TGF-β2 combined with CXCL4. (representative of n=3) **(E)** Transmission electron microscopy (TEM) images showing the high-resolution structure and organization of collagen fibers in the ECM produced by HC in medium control (upper panel) or after stimulation with TGFβ2 plus CXCL4 (lower panel). Black arrows depict dense bundles of collagen fibers observed in TGFβ2 plus CXCL4 treated fibroblasts. Scale bars are 2 μm and 1 μm for the left and the right images in both conditions, respectively. **(F)** Representative IF staining with collagen hybridizing peptide (CHP) (purple) for denatured collagen, hLAIR-1-IgG fusion protein (red) and DAPI (blue) on ECM produced by HC in medium condition or after stimulation with TGFβ2 combined with CXCL4 (n=4). Representative IF images were acquired on a confocal microscope with a 20x magnification. Results are represented as mean with SD. Differences were considered statistically significant when $*p < 0.05$ (Mann–Whitney test HC vs SSc patients groups, paired samples tested with RM one-way ANOVA, followed by Fisher's LSD). Results are represented as mean with SD.

Figure 3. PDGF receptor signaling and Matrix Metalloproteinases are required for deposition of fibrotic LAIR-1 binding structures. (A) HC fibroblasts were stimulated with TGF-β2 combined with CXCL4 and imaged during 6 days on a Incucyte live system. Representative phase contrast images (4x magnification) are shown (n=3). HC fibroblasts stimulated with TGF-β2 in combination with CXCL4 **(B)** in the presence or absence of 1 μM PDGF receptor inhibitor (Crenolanib) (n=4) or **(C)** in the presence of 100 μM MMP inhibitor (GM-6001) or DMSO as negative control (n=6). Samples were stained for immunofluorescence with hLAIR-1-gG fusion protein (red) and pan collagen antibodies (green). Immunofluorescence images were acquired on Incucyte using a 10x magnification and representative tiles of 16 images 4x4 are shown. The area (μm^2) of hLAIR-1-IgG plaques is quantified. Statistically significant differences were considered when $**p < 0.01$ (paired-t test).

Figure 4. Fibrotic disorganized collagen products have impaired capacity to activate LAIR-1. (A) Fluorescent hLAIR 1-IgG binding and **(B)** LAIR-1 response using a NFAT GFP reporter cell line transfected with hLAIR-1 and CD3ζ chimera (hLAIR-1-CD3ζ) to plate bound purified human Collagen I, gelatin from bovine skin and BSA (bovine serum albumin) as unspecific control (shown in blue shade). **(C)** Response (% of GFP+ cells measured by flow cytometry) of hLAIR-1-CD3ζ or control WT-CD3ζ parental cells to a mouse IgG1 isotype control (negative control), anti-LAIR-1 agonistic mAb (clone Dx26) (positive control), human purified collagen I (5 µg/mL), gelatin from bovine skin (5 µg/mL) and **(D)** to ECM produced by dermal HC dermal fibroblasts unstimulated or upon stimulation with TGFβ2 plus CXCL4 during 13 days (n=6). **(E)** hLAIR1-CD3ζ reporter cells were incubated on ECM produced by SSc patients (n=4) and HC (n=4) dermal fibroblasts unstimulated or upon stimulation (6 days) with TGFβ2 combined with CXCL4 and GFP expression (represented in green) was evaluated on the Incucyte imaging system during 70 hours. Paired samples were used to immunofluorescence staining for hLAIR-1-gG fusion protein (red), pan collagen antibodies (green) and DAPI (blue) to confirm the deposit of LAIR-1- binding ECM structures. Differences were considered statistically significant when *$p < 0.05$ (paired-t test).

Figure 5. Absence of LAIR-1 leads to increased bleomycin-induced skin fibrosis in the SSc mouse model. (A) WT or *Lair1*$^{-/-}$ mice were subcutaneously injected with bleomycin (BLM) or saline (NaCl) control for 2 weeks or 4 weeks. **(B)** Skin thickness was measured by caliper in unchallenged WT or *Lair1*$^{-/-}$ mice (36 mice per group, 3 independent experiments). **(C)** Caliper skin thickness and **(D)** collagen content was determined after 2 weeks of treatment (6 mice per group, 1 independent experiment). In the 4 weeks treatment model **(E)** caliper skin thickness (21-23 mice per group, 4 independent experiments) and **(F)** collagen content was measured (9-11 mice per group, 2 independent experiments). From the affected skin, **(G)** representative images of Masson's trichrome staining of affected skin and **(H)** quantification (n=6 per group, 1 independent experiment) are shown, as well as **(I)** representative histological αSMA staining (n=6 per group, 1 independent experiment). Data are shown as mean ± SD. Statistically significant differences were considered when *$p < 0.05$, **$p < 0.01$, ***$p < 0.001$ (Mann–Whitney test WT vs *Lair1*$^{-/-}$ groups).

Fig.1

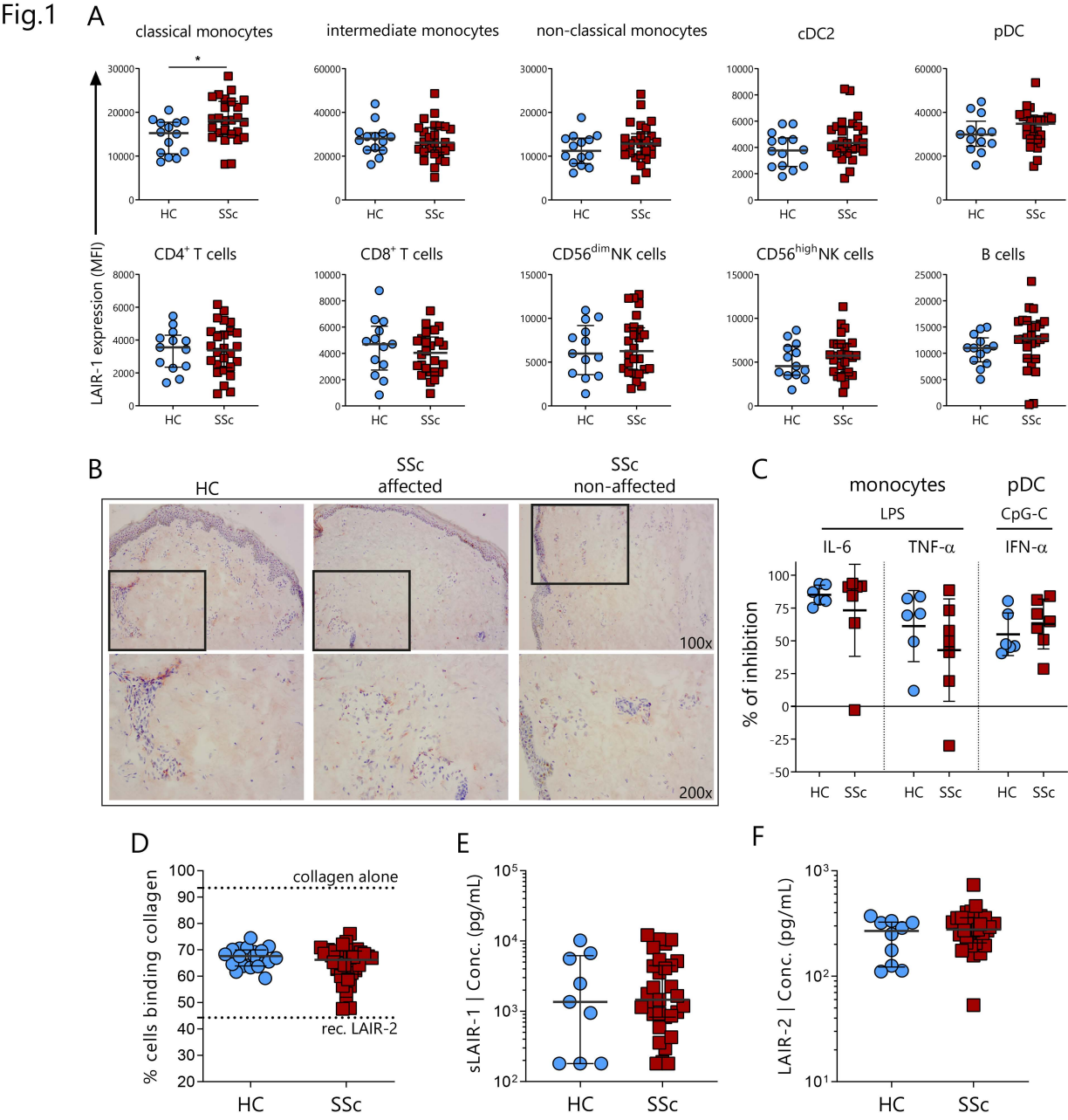
A
classical monocytes
intermediate monocytes
non-classical monocytes
cDC2
pDC
CD4+ T cells
CD8+ T cells
CD56dim NK cells
CD56high NK cells
B cells
LAIR-1 expression (MFI)
HC
SSc
B
HC
SSc affected
SSc non-affected
100x
200x
C
monocytes
pDC
LPS
CpG-C
IL-6
TNF-α
IFN-α
% of inhibition
D
collagen alone
rec. LAIR-2
% cells binding collagen
E
sLAIR-1 | Conc. (pg/mL)
F
LAIR-2 | Conc. (pg/mL)

Fig.2

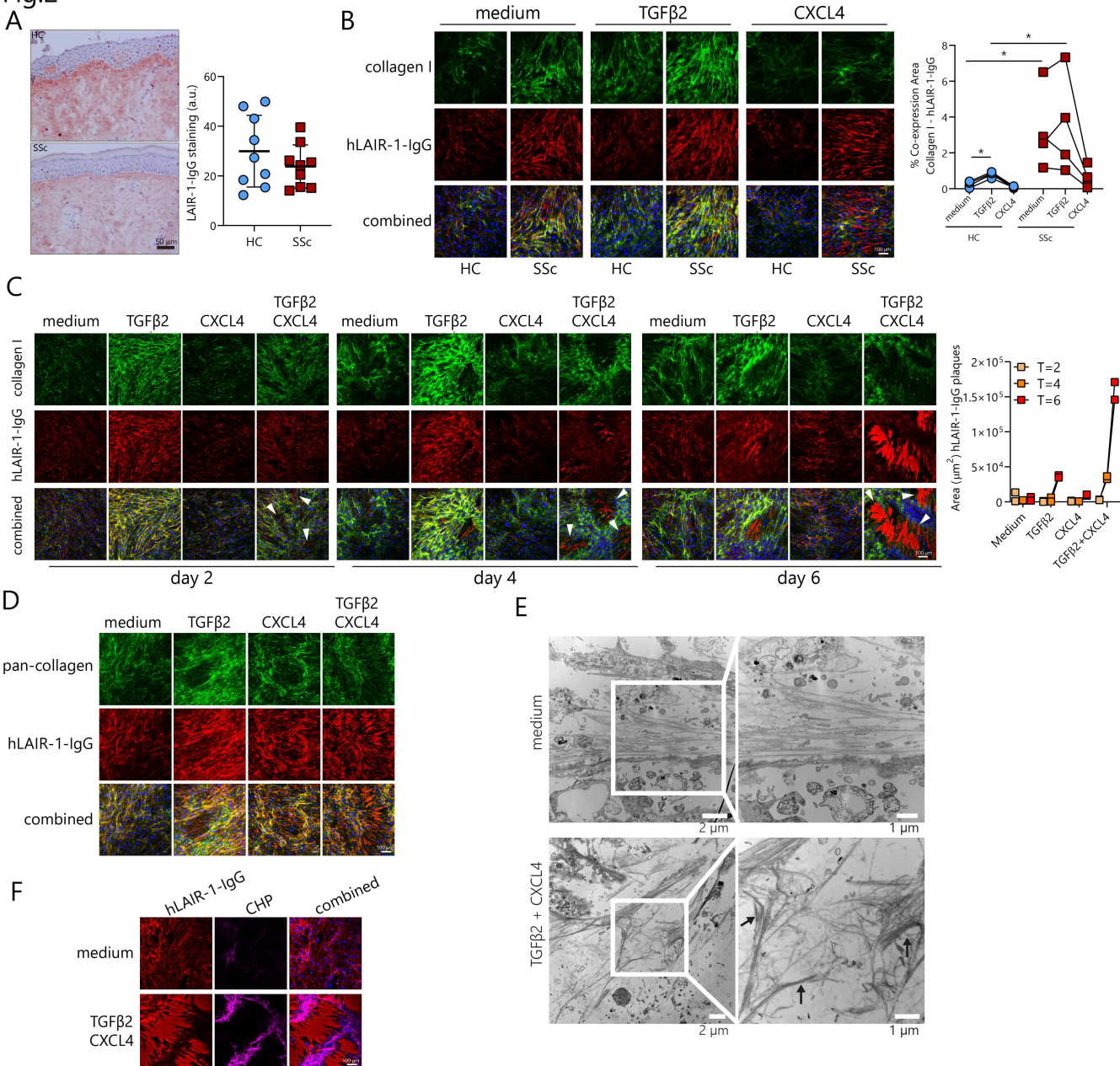
A
HC
SSc
50 µm
LAIR-1-IgG staining (a.u.)
60
40
20
0
HC
SSc
B
medium
TGFβ2
CXCL4
collagen I
hLAIR-1-IgG
combined
HC
SSc
HC
SSc
HC
SSc
100 µm
% Co-expression Area
Collagen I - hLAIR-1-IgG
8
6
4
2
0
*
*
*
medium
TGFβ2
CXCL4
medium
TGFβ2
CXCL4
HC
SSc
C
medium
TGFβ2
CXCL4
TGFβ2
CXCL4
collagen I
hLAIR-1-IgG
combined
day 2
day 4
day 6
200 µm
Area (µm²) hLAIR-1-IgG plaques
2×10⁵
1.5×10⁵
1×10⁵
5×10⁴
0
T=2
T=4
T=6
Medium
TGFβ2
CXCL4
TGFβ2+CXCL4
D
medium
TGFβ2
CXCL4
TGFβ2
CXCL4
pan-collagen
hLAIR-1-IgG
combined
100 µm
E
medium
TGFβ2 + CXCL4
2 µm
1 µm
2 µm
1 µm
F
hLAIR-1-IgG
CHP
combined
medium
TGFβ2
CXCL4
100 µm

Fig.3

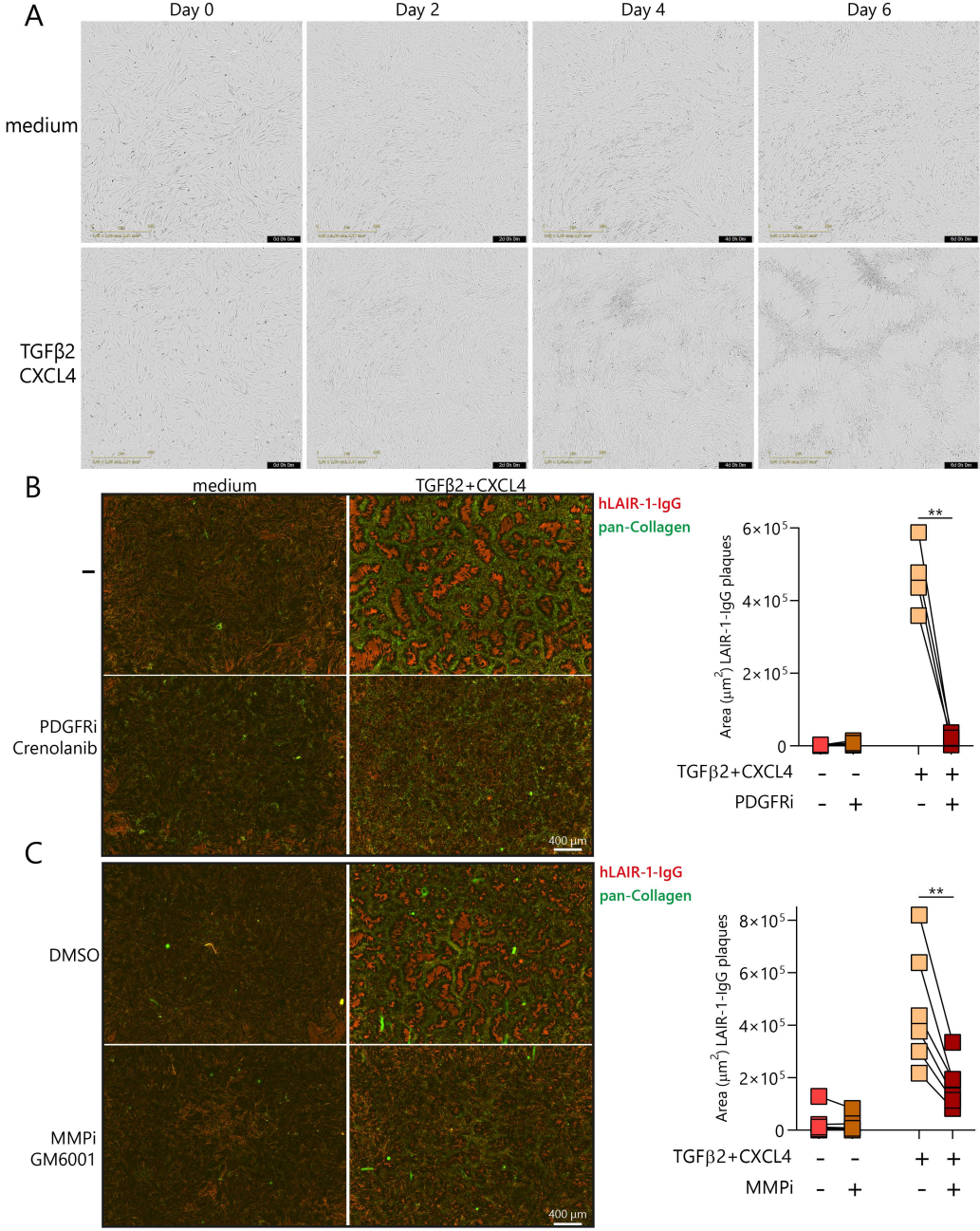
A
Day 0
Day 2
Day 4
Day 6
medium
TGFβ2
CXCL4
B
medium
TGFβ2+CXCL4
hLAIR-1-IgG
pan-Collagen
-
PDGFRi
Crenolanib
400 μm
Area (μm²) LAIR-1-IgG plaques
6×10⁵
4×10⁵
2×10⁵
0
**
TGFβ2+CXCL4 - - + +
PDGFRi - + - +
C
hLAIR-1-IgG
pan-Collagen
DMSO
MMPi
GM6001
400 μm
Area (μm²) LAIR-1-IgG plaques
8×10⁵
6×10⁵
4×10⁵
2×10⁵
0
**
TGFβ2+CXCL4 - - + +
MMPi - + - +

Fig.4

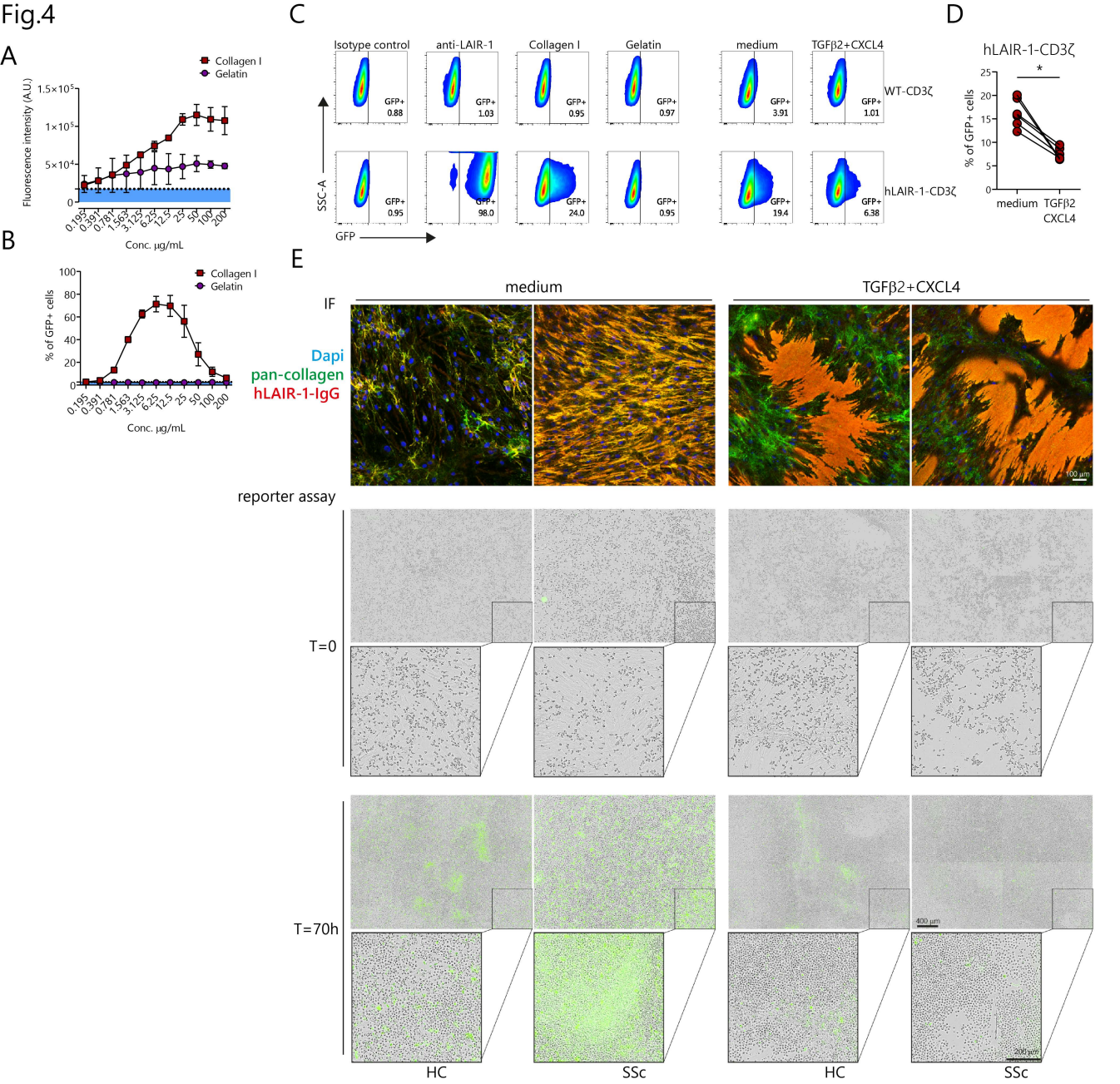
A
Collagen I
Gelatin
Fluorescence intensity (A.U.)
1.5×10^5
1×10^5
5×10^4
0
0.195
0.391
0.781
1.563
3.125
6.25
12.5
25
50
100
200
Conc. μg/mL
B
Collagen I
Gelatin
% of GFP+ cells
100
80
60
40
20
0
0.195
0.391
0.781
1.563
3.125
6.25
12.5
25
50
100
200
Conc. μg/mL
C
Isotype control
anti-LAIR-1
Collagen I
Gelatin
medium
TGFβ2+CXCL4
WT-CD3ζ
hLAIR-1-CD3ζ
SSC-A
GFP
GFP+ 0.88
GFP+ 1.03
GFP+ 0.95
GFP+ 0.97
GFP+ 3.91
GFP+ 1.01
GFP+ 0.95
GFP+ 98.0
GFP+ 24.0
GFP+ 0.95
GFP+ 19.4
GFP+ 6.38
D
hLAIR-1-CD3ζ
*
% of GFP+ cells
25
20
15
10
5
0
medium
TGFβ2 CXCL4
E
medium
TGFβ2+CXCL4
IF
Dapi
pan-collagen
hLAIR-1-IgG
100 μm
reporter assay
T=0
T=70h
400 μm
200 μm
HC
SSc
HC
SSc

Fig.5

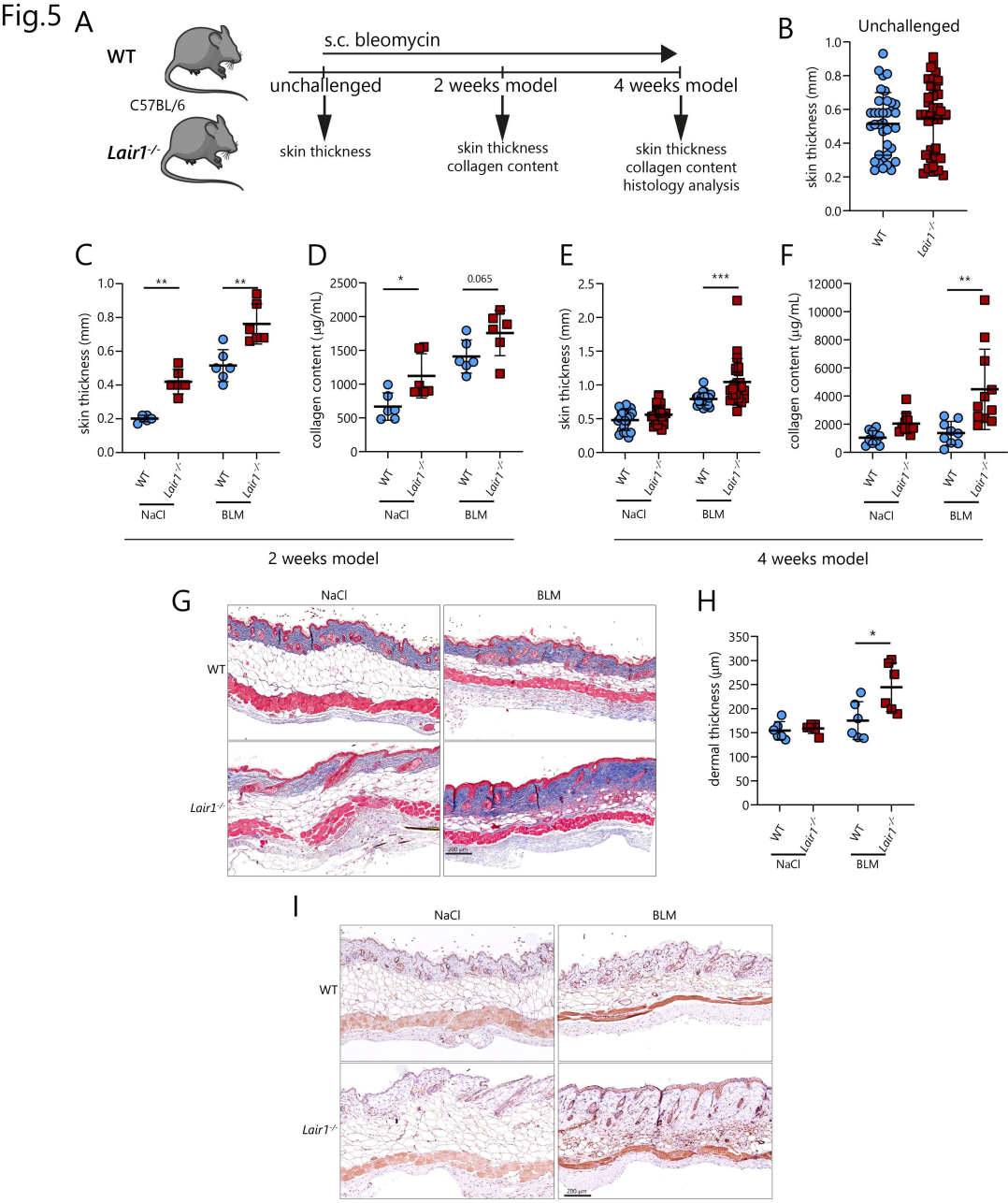
A
WT
C57BL/6
Lair1-/-
s.c. bleomycin
unchallenged
2 weeks model
4 weeks model
skin thickness
skin thickness
collagen content
skin thickness
collagen content
histology analysis
B
Unchallenged
skin thickness (mm)
WT
Lair1-/-
C
skin thickness (mm)
**
**
NaCl
BLM
D
collagen content (μg/mL)
*
0.065
E
skin thickness (mm)
***
F
collagen content (μg/mL)
**
2 weeks model
4 weeks model
G
NaCl
BLM
WT
Lair1-/-
200 μm
H
dermal thickness (μm)
*
I
NaCl
BLM
WT
Lair1-/-
200 μm